Received: 31 March 2022 | Revised: 20 June 2022 | Accepted: 4 July 2022 | Published on: 30 July 2022

DOI: 10.1002/mrm.29395

TECHNICAL NOTE

Magnetic Resonance in Medicine

Assessing potential correlation between T_2 relaxation and diffusion of lactate in the mouse brain

Eloïse Mougel | **Sophie Malaquin** | **Julien Valette**

Laboratoire des Maladies Neurodégénératives, Université Paris-Saclay, Commissariat à l'Energie Atomique et aux Energies Alternatives (CEA), Centre National de la Recherche Scientifique (CNRS), Molecular Imaging Research Center (MIRCen), Fontenay-aux-Roses, France

Correspondence
Julien Valette, Laboratoire des Maladies Neurodégénératives, Université Paris-Saclay, Commissariat à l'Energie Atomique et aux Energies Alternatives (CEA), Centre National de la Recherche Scientifique (CNRS), Molecular Imaging Research Center (MIRCen), 18 Route du Panorama, 92260 Fontenay-aux-Roses, France.
Email: julien.valette@cea.fr

Funding information
H2020 European Research Council, Grant/Award Number: 818266

Purpose: While diffusion and T_2 relaxation are intertwined, little or no correlation exists between diffusion and T_2 relaxation of intracellular metabolites in the rodent brain, as measured by diffusion-weighted MRS at different TEs. However, situation might be different for lactate, since it is present in both extracellular and intracellular spaces, which exhibit different diffusion properties and may also exhibit different T_2. Such a TE dependence would be crucial to account for when interpreting or modeling lactate diffusion. Here we propose to take advantage of a new diffusion sequence, where J-modulation of lactate is canceled even at long TE, thus retaining excellent signal, to assess potential T_2 dependence on diffusion of lactate in the mouse brain.

Methods: Using a frequency-selective diffusion-weighted spin-echo sequence that removes J-modulation at 1.3 ppm, thus preserving lactate signal even at long TE, we investigate the effect of TE between 50.9 and 110.9 ms (while keeping diffusion time constant) on apparent diffusivity and kurtosis in the mouse brain.

Results: Regardless of the metabolites, no difference appears for the diffusion-weighted signal attenuation with increasing TE. For lactate, apparent diffusivity and kurtosis remain unchanged as TE increases.

Conclusion: No significant TE dependence of diffusivity and kurtosis is measured for lactate in the 50–110 ms TE range, confirming that potential T_2 effects can be ignored when interpreting or modeling lactate diffusion.

KEYWORDS

apparent diffusivity, apparent kurtosis, compartmentation, DW-MRS, frequency-selective sequence, intracellular/extracellular, lactate, T_2 relaxation

1 | INTRODUCTION

Diffusion-weighted MRS (DW-MRS) is sensitive to the microstructure of the environment where metabolites are diffusing.[1] In parallel, microstructure and diffusion also influence the relaxation time T_2, so that T_2 and diffusion might be correlated, i.e., diffusion properties as measured with DW-MRS may depend on the TE. In white matter, biophysical models[2] used to estimate water diffusivity require taking into account both compartment-specific diffusion properties and compartment-specific T_2. Such a TE-dependency of water apparent diffusivity has been

observed previously in gray matter at 1.5T in human brain over a 54–130 ms TE range,[3] and in ex-vivo rat brain at 14.0T over a 24.2–100 ms TE range.[4] In other words, due to differences in compartmental T_2 values,[2] with in particular extracellular $T_2 \sim 1.5$-fold longer than intracellular T_2, the ADC of extracellular water over-contributes to total water ADC when increasing TE.

Things seems to be simpler for intracellular metabolites in the mouse brain (mostly gray matter), where it was shown by Ligneul et al.[5] that signal attenuation is fundamentally unchanged when increasing TE from 33.4 ms to 73.4 ms (although N-acetylaspartate attenuation seemed to exhibit slight TE-dependency at the highest diffusion weighting [*b*-values], i.e., for $b = 20$ and 30 ms/μm^2). Nevertheless, the situation might be different for lactate, which is present in both intracellular and extracellular space,[6] two compartments which appear to have quite distinct diffusion properties,[7] and where T_2 could also be different, like for water. This TE dependence could be an important point to investigate in the perspective of modeling DW-MRS data to determine lactate fraction in the different compartments in gray matter.[8] However, this issue has been eluded so far, due to the difficulty of measuring lactate diffusion, even more so when TE is increased.

Here, we use our recent frequency-selective DW-spin-echo (DW-SE) sequence,[9] where TE can be changed while canceling J-modulation on the CH_3 lactate peak, thus preserving signal even at long TE. With this approach, we are able to measure apparent diffusivity and kurtosis of lactate for TE ranging from 50 to 110 ms in the mouse brain.

2 | METHODS

All experimental protocols were reviewed and approved by the local ethics committee (CETEA N°44), and authorized by the French Ministry of Education and Research. They were performed in an approved facility (authorization #B92-032-02), in strict accordance with recommendations of the European Union (2010-63/EEC). All efforts were made to minimize animal suffering, and animal care was supervised by veterinarians and animal technicians. Mice were housed under standard environmental conditions (12-h light–dark cycle, temperature: 22 ± 1°C and humidity: 50%) with ad libitum access to food and water.

Experiments were performed on an 11.7 T BioSpec Bruker scanner interfaced to PV6.0.1 (Bruker, Ettlingen, Germany). A quadrature surface cryoprobe (Bruker, Ettlingen, Germany) was used for transmission and reception. Six C57BL/6 mice were anesthetized with ∼1.5% isoflurane and maintained on a stereotaxic bed with a bite and two ear bars. Throughout the experiments, body temperature was monitored and maintained at ∼36°C by warm water circulation. Breathing frequency was monitored using PC–SAM software (Small Animal Instruments, Inc., Stony Brook, NY).

A 13.2-μL ($3.3 \times 2 \times 2$ mm^3) spectroscopic voxel was placed in the striatum in such a way that CSF contamination was minimal (<1%, as evaluated on anatomical images acquired with a RARE sequence with TE/TR = 30/2500 ms, 78.1-μm isotropic resolution and 0.5-mm slice thickness, using manual segmentation with the Fiji distribution of the ImageJ software). Shimming was performed using Bruker's Mapshim routine, yielding a water linewidth of ∼17 Hz. DW-MRS acquisitions were performed using a spectrally-selective DW-SE-LASER sequence, where the SE part incorporates a 5-ms single-band spectrally selective refocusing pulse,[9] followed by LASER localization. The duration of the diffusion gradients was set to $\delta = 3.6$ ms. Diffusion gradients were positioned around the spectrally-selective refocusing pulse, and separated by a delay $\Delta = 21.2$ ms, resulting in diffusion time $t_d = 20$ ms. Signal attenuation of N-acetylaspartate (NAA), choline compounds (tCho), creatine + phosphocreatine (tCr), taurine (Tau), and lactate (Lac) was measured for $b = [0.02, 1.2, 3.02, 6]$ ms/μm^2, at different TE = [50.9, 66.9, 86.9, 110.9] ms which were obtained by varying the delays before and after the diffusion gradients, i.e., keeping t_d constant (as well as the TE of the LASER part, and TR = 2 s). Due to their low signal especially at long TE, signal attenuation of other metabolites was not measured. Two sets of 32 repetitions were acquired for TE = 50.9, 66.9 and 86.9 ms; and three sets of 32 repetitions were acquired for TE = 110.9 ms to improve signal-to-noise ratio. The spectrally-selective pulse is generated to refocus the 0.1–4.0 ppm range, thus avoiding refocusing the 4.1-ppm CH lactate group coupled to the 1.3-ppm CH_3, resulting in suppression of J-modulation. Because of such frequency selectivity, no water suppression is required with this sequence. In addition, the diffusion gradient direction was changed at each repetition to perform powder-averaging corresponding to 32 different gradient directions, and the phase cycling was implemented to have a new phase at each new direction.

Individual scans were frequency- and phased-corrected before averaging, and spectra were analyzed with LCModel.[10] Experimental MM spectra, acquired for each TE using a double inversion recovery module ($TI_1 = 2200$ ms and $TI_2 = 770$ ms) at $b = 10$ ms/μm^2 to remove potential residual metabolite signal, were included in LCModel basis-sets.

Signal attenuations were fitted over the whole *b*-range (corresponding to a low *b*-regime, within the convergence radius of the cumulant expansion[11]) to estimate the mean diffusivity and mean kurtosis, using the following

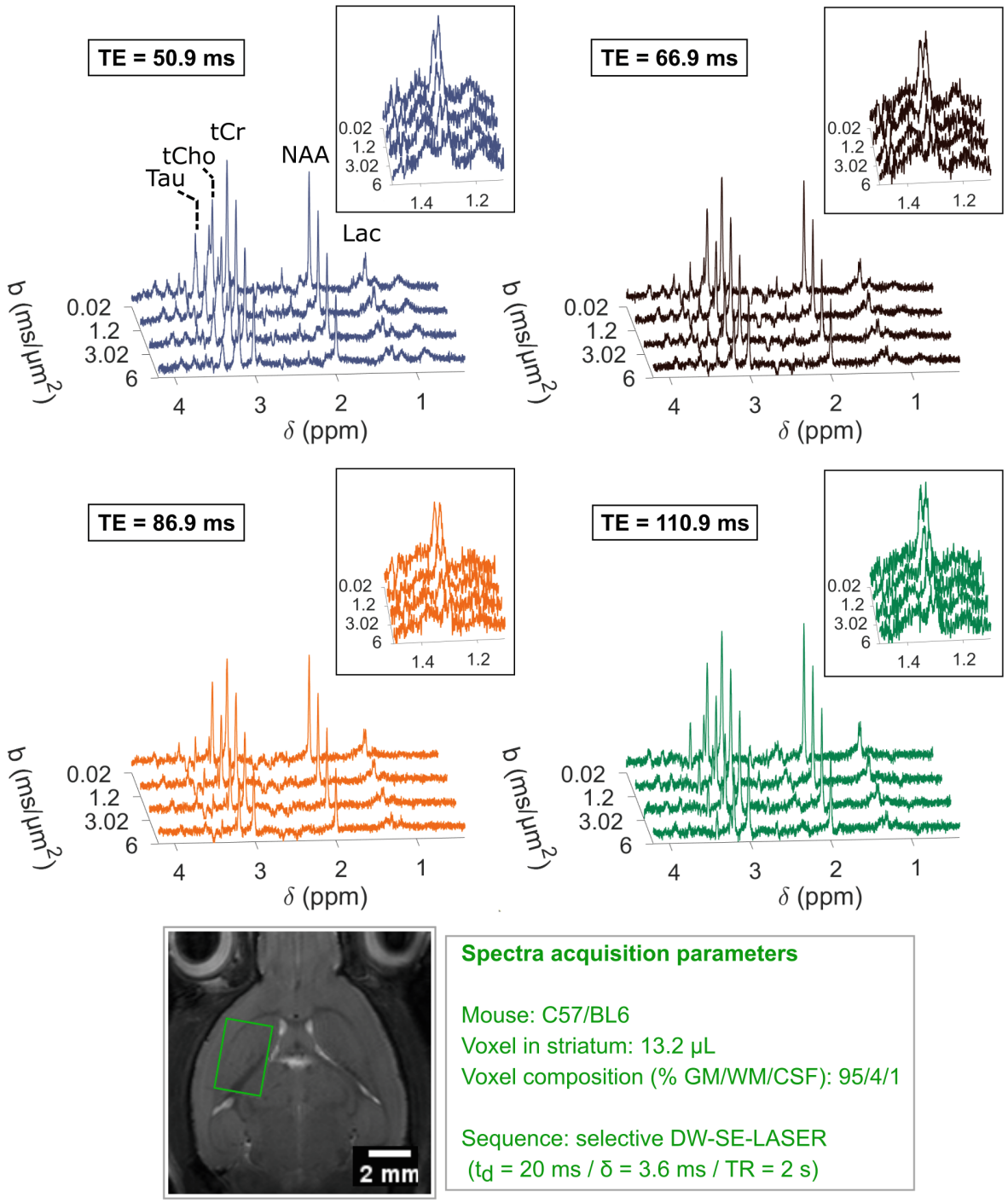

FIGURE 1 Example of spectra at different diffusion-weightings, acquired in a 13.2-μL voxel (bottom image) in the striatum of a single mouse at different TEs (while keeping constant t_d = 20 ms). The contribution of CSF and white matter is <1% and <4% in the voxel of interest, respectively. The spectra at TE = 110.9 ms were acquired with 3 × 32 repetitions versus 2 × 32 repetitions for other TE (hence, the apparent larger signal and noise at TE = 110.9 ms). Lactate is still visible at the highest *b*-value

equation[12]:

$$S(b) = S(b=0) \times exp\left(-b\,D_{app} + \frac{1}{6}\,K_{app}\,\left(b\,D_{app}\right)^2\right) \quad (1)$$

with D_{app} the apparent diffusivity (that we will use interchangeably with "ADC") and K_{app} the apparent kurtosis.

Finally, statistical analysis was performed, with open-source software JASP (Version 0.16.0), using a one-way repeated-measures analysis of variance (ANOVA) to compare the D_{app} and K_{app} values across the six mice between TE. We checked for each repeated-measures ANOVA the sphericity assumption with a Maulchy's

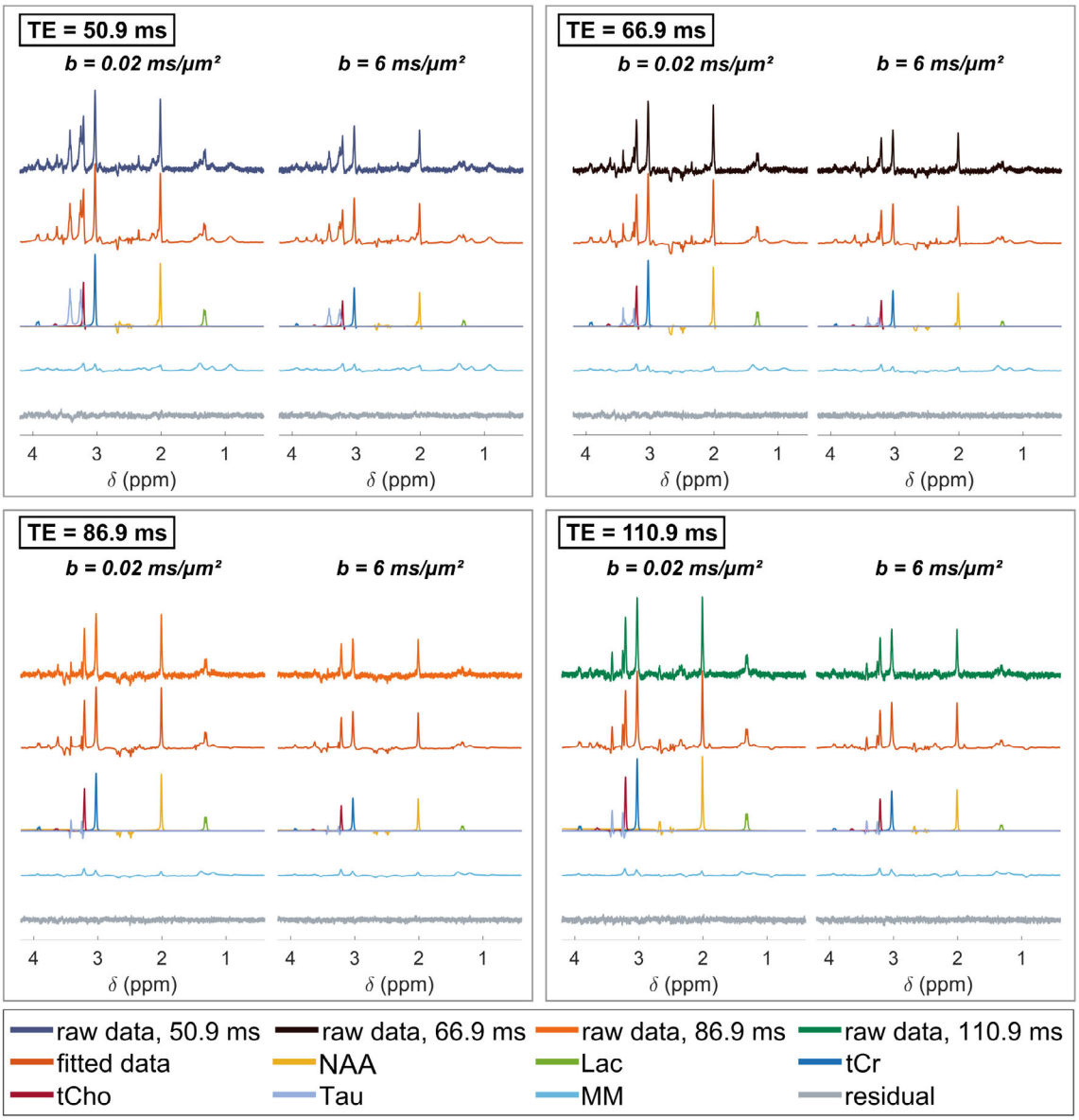

FIGURE 2 Example of LCModel analysis at different diffusion-weightings and different TE, for data acquired in one mouse. For lactate, the Cramér-Rao lower bound (CRLB) is ~7% in the worst condition (largest *b*-value for TE = 110.9 ms), and the average CRLB over all *b*-value and TE for this mouse is ~4%. Average CRLB is ~2% for NAA, ~1% for tCr, ~2% for tCho, ~4% for Tau. The signal at TE = 110.9 ms appears just as high as at TE = 50.9 ms, due to the number of repetitions, which is 3 × 32 for TE = 110.9 ms and 2 × 32 for TE = 50.9 ms.

test. A post hoc test with Bonferroni correction was then performed to assess the inter TE significance.

3 | RESULTS

The frequency-selective DW-SE sequence allows measuring lactate peak without J-modulation, regardless of TE. We observe (Figure 1) that the lactate peak is clearly visible on spectra even at long TE and for the largest *b*-value, despite the small voxel size. Such signal allows acceptable LCModel estimation (Figure 2) with CRLBs <10% in the worst condition ($b = 6\,\text{ms}/\mu\text{m}^2$ and TE = 110.9 ms). This highlights the interest of using the frequency-selective DW-SE sequence in the context of this study. Nevertheless, as already noted previously,[9] the myo-inositol peak (~3.5 ppm) is quite low due to its location on the transition band of the spectrally-selective pulse (width ~ 0.9 ppm giving an inversion of only ~80%), resulting in relatively large quantification errors. Here myo-inositol signal is much smaller and could not be quantified properly at high *b*-value. We thus ignore it in the rest of this paper.

Visually, lactate signal attenuation over six mice appears to be quite similar for the different TE. Overall, this seems to be also the case for the other metabolites (Figure 3). Despite the efficiency of the sequence to

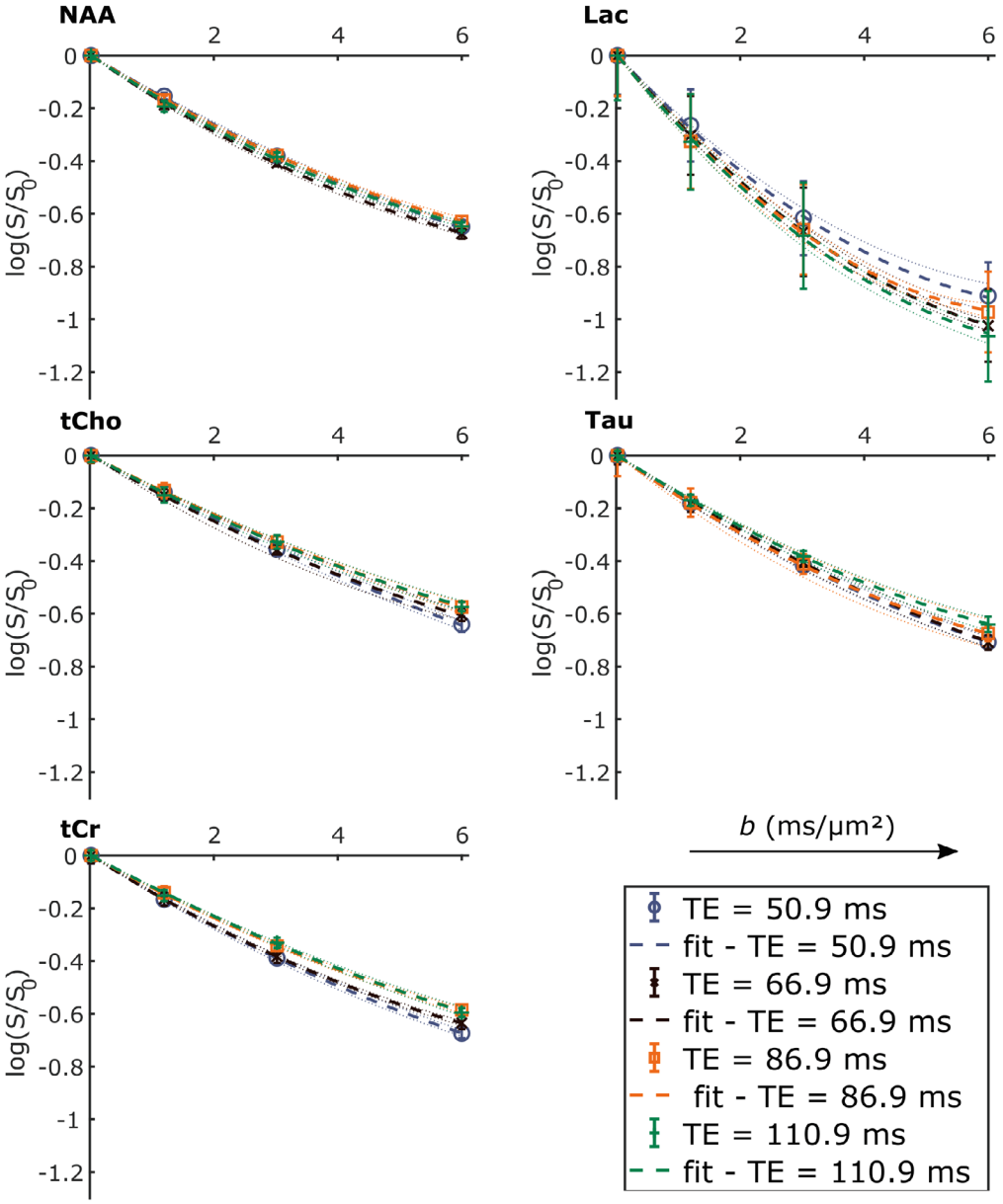

FIGURE 3 Average measured signal attenuation and standard error of the mean (dot) for each metabolite over six mice for different diffusion times; average fit using Equation (1) (dashed line); and standard error of the mean of the fit (dotted line) over six mice overlaid on the same graph. Signal attenuations are similar regardless of TE. In this example, for all metabolites the model given by Equation (1) fits the data well

measure lactate, the standard error of the mean remains larger for lactate than for NAA or other more concentrated metabolites.

In the range of *b*-values chosen for this study, Equation (1) seems to correctly fit signal attenuation, as represented for example with the dashed lines in Figure 3. Corresponding D_{app} and K_{app} values (Figure 4) exhibit no significant change (calculated with a repeated-measures ANOVA) when increasing TE in the 50–110 ms range for all metabolites, except for tCr, which exhibits a slightly decreasing D_{app}. For intracellular metabolites, D_{app} is in the range [0.11; 0.16] $\mu m^2/ms$ at all TE, while K_{app} remains in the range [1.1; 1.9]. For lactate, the kurtosis (~1.4) is constant and in the same range as for the other metabolites. Lactate diffusion (~0.25 $\mu m^2/ms$) is higher than for other metabolites, suggesting some impact of extracellular lactate with faster diffusivity, but no significant TE-effect is observed on these diffusion parameters.

4 | DISCUSSION

4.1 | ADC estimates in line with the literature

Despite difference in methodologies to estimate ADCs, our measurements (~0.15 $\mu m^2/ms$) are of the same order of magnitude as those previously reported in the literature (~0.1 $\mu m^2/ms$ using a DW-stimulated echo sequence + monoexponential fitting in a [0; 5] $ms/\mu m^2$ *b*-value range)[5] in the mouse brain for NAA, tCr, tCho, and Tau. Actually, considering the ~2-fold shorter diffusion time

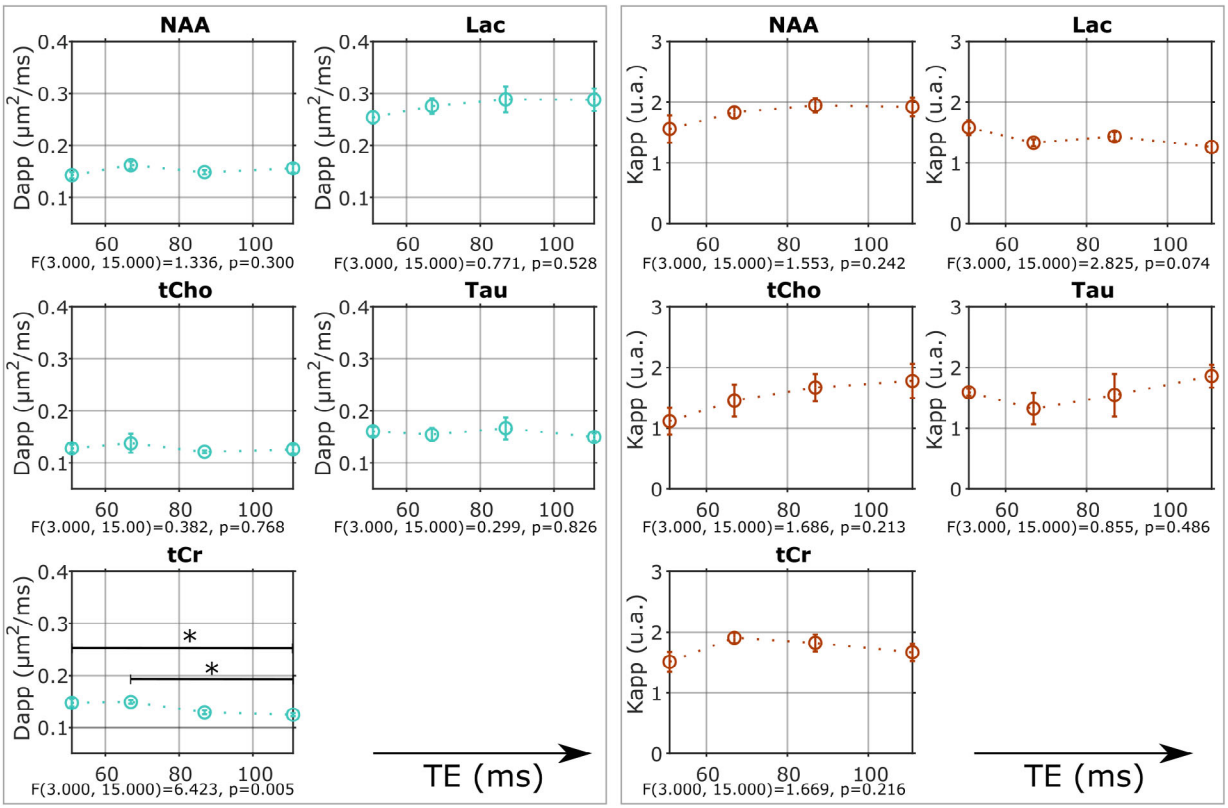

FIGURE 4 Average apparent diffusivity D_{app} and kurtosis K_{app} extracted from metabolite signal attenuation as a function of TE. Left: D_{app} is plotted as a function of TE. Repeated-measures ANOVA (reported by the F-test result below each graph) shows no significant variation except for tCr (*: $p < 0.05$ pairwise post hoc test with Bonferroni correction). Right: K_{app} is plotted as a function of TE. No significant variation is noted

used here (t_d = 20 ms versus t_d = 63 ms), our estimate of intracellular ADC is consistent with the increase in ADC as t_d decreases for relatively short t_d.[13] Lactate ADC being ~70% larger than intracellular metabolite ADC presumably mostly reflects some extracellular contribution,[7] although lactate is also a smaller molecule with ~30% larger intrinsic diffusivity.

4.2 | Lactate kurtosis measurements

To our knowledge, this study reports for the first time the measurement of kurtosis for lactate. Kurtosis appears quite similar between metabolites and is in line with our previous measurements for intracellular metabolites.[14] Hence lactate K_{app} appears to be less influenced by extracellular contribution than D_{app}.

4.3 | No TE-dependence of lactate diffusion

In gray matter, for TEs ranging from 50 to 110 ms, no dependence of diffusion on TE is observed for lactate, as for almost all intracellular metabolites. To assess overall dependence on TE, a repeated-measures ANOVA is more relevant than a paired-samples t-test, nevertheless, a paired-samples t-test is sensitive to a 2-fold smaller difference than such ANOVA and could detect a difference of at least 15% (assessed a posteriori by Monte Carlo simulation for $p < 0.05$). As shown in Table 1, even with the t-test sensitive to a smaller difference, no TE dependence is noted for lactate apparent diffusivity, and only one small difference (p-value = 0.04) is observed for apparent kurtosis between 50 ms and 67 ms, with the other comparisons clearly not significantly different (p-value >0.1). This therefore suggests the lack of a highly significant TE-dependence of diffusion for lactate, with a threshold of 15% difference on the diffusion parameters. These observations corroborate, over a wider TE range, previous measurements reported by Ligneul et al.[5] for intracellular metabolites. Considering that lactate is present in both intracellular and extracellular spaces, and that intra- and extracellular diffusion properties are expected to be quite different based on the latest works,[7] lack of TE-dependence for diffusion suggests that T_2s are not sufficiently different in both compartments for diffusion measurements to exhibit TE-dependency. Another way to

TABLE 1 *p*-value obtained with two different analyses (repeated-measures ANOVA [RMANOVA] and paired-samples t-test) for D_{app} and K_{app} for lactate (†: $p < 0.05$ paired-samples t-test)

		***p*-Value**					
Param	**Test**	**TE(50)-TE(67)**	**TE(50)-TE(87)**	**TE(50)-TE(111)**	**TE(67)-TE(87)**	**TE(67)-TE(111)**	**TE(87)-TE(111)**
D_{app}	RMANOVA	0.528					
	paired-samples t-test	0.41	0.266	0.308	0.702	0.631	0.971
K_{app}	RMANOVA	0.074					
	paired-samples t-test	**0.044** (†)	0.304	0.112	0.333	0.533	0.127

Note : The repeated-measures ANOVA is the most appropriate test to assess whether a significant dependence of TE exists on diffusion parameters, nevertheless the paired-samples t-test is sensitive to a 2-fold smaller difference, (i.e., 15% D_{app} or K_{app} for lactate) (a posteriori estimation with Monte Carlo simulation for a paired-samples t-test and 95% confidence interval of the mean for RMANOVA). Although the paired-samples t-test would pick up lower difference, the results still do not exhibit significant difference for diffusion properties, except for the pairwise comparison between 50 ms and 67 ms for K_{app} (with a *p*-value ~ 0.044).

look at it is that, despite lactate diffusion being quite different between compartments (as evidenced by the ADC higher than for purely intracellular metabolites, or suggested by other works[7,8]), microstructural differences do not influence T_2[15,16] to a large enough extent to produce detectable differences at the time scale of our experiment. Therefore, DW-MRS measurements are robust over such a wide range of TE, and diffusion models only considering diffusion properties in the different compartments (as well as potential inter-compartment exchange[17,18]), without considering differences in T_2, should be valid to model lactate diffusion.

4.4 | tCr: specific behavior or artifact?

The small decrease in tCr apparent diffusivity remains of uncertain origin. Due to the different sizes for Cr and PCr, their D_{app} and T_2 could be different enough to induce variability in tCr diffusivity. Nevertheless, since their spectra are very close at 11.7T except for the peaks at ~3.9 ppm, it is difficult to discriminate the contributions of Cr and PCr using the spectrally selective SE sequence, because these 3.9-ppm peaks fall on the edge the transition band of the pulse (~18% inversion at 3.9 ppm), thus yielding almost no signal. The slight decrease of tCr D_{app} with increasing TE thus remains an open question. Interestingly, such behavior was reported in the human white matter, but at much longer diffusion time; at diffusion time closer to the one of the present study, the opposite behavior (ADC of tCr increasing with TE) was reported.[19]

5 | CONCLUSIONS

Using a frequency-selective DW-SE sequence, which allows measuring lactate diffusion without J-modulation, we measured signal attenuation of lactate and other metabolites for different TE in the 50–110 ms range (while keeping diffusion delays constant), in a small voxel in the mouse brain. These measurements revealed no effect of TE on diffusion, neither for most intracellular metabolites, nor for lactate, which is in both intra and extracellular compartments. This suggests that lactate T_2 in the intra and extracellular compartments is not sufficiently different to induce TE-dependency of measured diffusion properties. This in turn suggests that lactate diffusion can be modeled by considering only diffusion properties in the different compartments (as well as potential exchange), without taking into account relaxation effects.

ACKNOWLEDGMENTS

This project has received funding from the European Research Council (ERC) under the European Union's Horizon 2020 research and innovation programmes (grant agreement No 818266). The 11.7 T MRI scanner was funded by a grant from "Investissements d'Avenir - ANR-11-INBS-0011 - NeurATRIS: A Translational Research Infrastructure for Biotherapies in Neurosciences".

ORCID

Julien Valette https://orcid.org/0000-0002-2067-5051

REFERENCES

1. Ronen I, Valette J. Diffusion-weighted magnetic resonance spectroscopy. *eMagRes*. 2015;4:733-750.
2. Veraart J, Novikov DS, Fieremans E. TE dependent diffusion imaging (TEdDI) distinguishes between compartmental T2 relaxation times. *Neuroimage*. 2018;182:360-369.
3. Vestergaard-Poulsen P, Hansen B, Østergaard L, Jakobsen R. Microstructural changes in ischemic cortical gray matter predicted by a model of diffusion-weighted MRI. *J Magn Reson Imaging*. 2007;26:529-540.

4. Buckley DL, Bui JD, Phillips MI, et al. The effect of ouabain on water diffusion in the rat hippocampal slice measured by high resolution NMR imaging. *Magn Reson Med*. 1999;41:137-142.
5. Ligneul C, Palombo M, Valette J. Metabolite diffusion up to very high b in the mouse brain in vivo: revisiting the potential correlation between relaxation and diffusion properties. *Magn Reson Med*. 2017;77:1390-1398.
6. Mächler P, Wyss MT, Elsayed M, et al. In vivo evidence for a lactate gradient from astrocytes to neurons. *Cell Metab*. 2016;23:94-102.
7. Vincent M, Gaudin M, Lucas-Torres C, Wong A, Escartin C, Valette J. Characterizing extracellular diffusion properties using diffusion-weighted MRS of sucrose injected in mouse brain. *NMR Biomed*. 2021;34:e4478.
8. Pfeuffer J, Tkác I, Gruetter R. Extracellular-intracellular distribution of glucose and lactate in the rat brain assessed noninvasively by diffusion-weighted 1H nuclear magnetic resonance spectroscopy in vivo. *J Cereb Blood Flow Metab*. 2000;20:736-746.
9. Mougel E, Malaquin S, Vincent M, Valette J. Using spectrally-selective radiofrequency pulses to enhance lactate signal for diffusion-weighted MRS measurements in vivo. *J Magn Reson*. 2022;334:107113.
10. Provencher SW. Automatic quantitation of localized in vivo 1H spectra with LCModel. *NMR Biomed*. 2001;14:260-264.
11. Frøhlich AF, Østergaard L, Kiselev VG. Effect of impermeable boundaries on diffusion-attenuated MR signal. *J Magn Reson*. 2006;179:223-233.
12. Jensen JH, Helpern JA. Quantifying non-Gaussian water diffusion by means of pulsed-field-gradient MRI. *Proc Intl Soc Mag Reson Med*. 2003;13:2154.
13. Valette J, Ligneul C, Marchadour C, Najac C, Palombo M. Brain metabolite diffusion from ultra-short to ultra-long time scales: what do we learn, where should we go? *Front Neurosci*. 2018;12:2.
14. Mougel E, Valette J, Palombo M. Investigating exchange, structural disorder and restriction in gray matter via water and metabolites diffusivity and kurtosis time-dependence. *Proc Intl Soc Mag Reson Med*. 2022;31:255.
15. Michaeli S, Garwood M, Zhu XH, et al. Proton T2 relaxation study of water, N-acetylaspartate, and creatine in human brain using Hahn and Carr-Purcell spin echoes at 4T and 7T. *Magn Reson Med*. 2002;47:629-633.
16. Kiselev VG, Novikov DS. Transverse NMR relaxation in biological tissues. *Neuroimage*. 2018;182:149-168.
17. Lee HH, Papaioannou A, Novikov DS, Fieremans E. In vivo observation and biophysical interpretation of time-dependent diffusion in human cortical gray matter. *Neuroimage*. 2020;222:117054.
18. Palombo M, Shemesh N, Ronen I, Valette J. Insights into brain microstructure from in vivo DW-MRS. *Neuroimage*. 2018;182:97-116.
19. Branzoli F, Ercan E, Webb A, Ronen I. The interaction between apparent diffusion coefficients and transverse relaxation rates of human brain metabolites and water studied by diffusion-weighted spectroscopy at 7 T. *NMR Biomed*. 2014;27:495-506.

How to cite this article: Mougel E, Malaquin S, Valette J. Assessing potential correlation between T_2 relaxation and diffusion of lactate in the mouse brain. *Magn Reson Med*. 2022;88:2277-2284. doi: 10.1002/mrm.29395